Observed forest sensitivity to climate implies large changes in 21st century North American forest growth

Noah D. Charney, Flurin Babst, Benjamin Poulter, Sydne Record, Valerie M. Trouet, David Frank, Brian J. Enquist, and Margaret E. K. Evans

LETTER

Observed forest sensitivity to climate implies large changes in 21st century North American forest growth

Noah D. Charney,[1]*
Flurin Babst,[2,3,4] Benjamin Poulter,[5]
Sydne Record,[6] Valerie M. Trouet,[2]
David Frank,[3] Brian J. Enquist[1,7,8]
and Margaret E. K. Evans[2]

Abstract

Predicting long-term trends in forest growth requires accurate characterisation of how the relationship between forest productivity and climatic stress varies across climatic regimes. Using a network of over two million tree-ring observations spanning North America and a space-for-time substitution methodology, we forecast climate impacts on future forest growth. We explored differing scenarios of increased water-use efficiency (WUE) due to CO_2-fertilisation, which we simulated as increased effective precipitation. In our forecasts: (1) climate change negatively impacted forest growth rates in the interior west and positively impacted forest growth along the western, southeastern and northeastern coasts; (2) shifting climate sensitivities offset positive effects of warming on high-latitude forests, leaving no evidence for continued 'boreal greening'; and (3) it took a 72% WUE enhancement to compensate for continentally averaged growth declines under RCP 8.5. Our results highlight the importance of locally adapted forest management strategies to handle regional differences in growth responses to climate change.

Keywords

Climate change, dendrochronology, forecasting, forests, growth, modelling, trees.

INTRODUCTION

Forests play a key role in coupled land–atmosphere exchange processes, which determine a range of ecosystem services (Bonan 2008; Carpenter *et al.* 2009). Changes in forest function with climate change are expected to feedback on the climate system at multiple spatiotemporal scales (Bonan 2008), as forests play a substantial role in mitigating anthropogenic greenhouse gas emissions (Pan *et al.* 2011). The fate of forests in a warming world is thus of major ecological, societal and economic concern. Evidence is mounting, however, that the global forest carbon sink may not be sustained in the future due to saturation effects (Nabuurs *et al.* 2013), increased drought- and disturbance-related tree mortality (Allen *et al.* 2010; McDowell *et al.* 2015; Millar & Stephenson 2015) and biome shifts that may counteract the positive effect of rising temperatures on boreal forest growth (Williams *et al.* 2011; Piao *et al.* 2014). Existing models of forest growth dynamics include large uncertainties which ramify and lead to divergence in forecasts of how climate change will impact the future terrestrial carbon cycle (Keenan *et al.* 2012; Piao *et al.* 2013). To reduce these uncertainties, it is necessary to extend assessments of current observation networks using novel analytical approaches and data sources (Lindner *et al.* 2014).

A challenge for climate-impact modelling is assessing the contribution of uncertainty introduced by applying contemporary species-environment relationships to future climate conditions. Observed correlations between climate and growth rates at a given location are often used to estimate future growth rates at the same location. However, such estimates will include increasing inaccuracies as growth becomes constrained by different limiting factors under future climate conditions, for example, Liebig's Law of the Minimum (Albright & Peterson 2013). One way to address this challenge is to use a space-for-time substitution approach: future species-environment relationships at a given location are inferred from distant locations where the current climate resembles future climate at the focal location (Blois *et al.* 2013).

For plants, one key way that future conditions may differ from the past is the increased availability of atmospheric carbon. When forecasting responses to climate change, the degree to which increased atmospheric CO_2 might directly increase future plant growth, that is, 'carbon fertilisation' (van der Sleen *et al.* 2014; Farrior *et al.* 2015), remains an important unresolved effect. Increased atmospheric CO_2 may influence plant growth through several pathways and these effects are integrated within metrics of water-use efficiency (WUE; Ainsworth & Long 2005; Farrior *et al.* 2015). Increased WUE has been invoked to explain observations such as accelerated growth in free-air carbon enrichment experiments (Norby & Zak 2011), but its role in reducing water-stress is actively debated (Allen *et al.* 2015).

Here, we present a novel analytical pipeline, leveraging a continental-scale tree-ring network to forecast changes in

[1]*Department of Ecology and Evolutionary Biology, University of Arizona, Bioscience West, Tucson, AZ, USA*
[2]*Laboratory of Tree-Ring Research, University of Arizona, Tucson, AZ, USA*
[3]*Dendroclimatology, Swiss Federal Research Institute WSL, Birmensdorf, Switzerland*
[4]*W. Szafer Institute of Botany, Polish Academy of Sciences, Krakow, Poland*

[5]*Department of Ecology, Montana State University, Bozeman, MT, USA*
[6]*Department of Biology, Bryn Mawr College, Bryn Mawr, PA, USA*
[7]*Santa Fe Institute, Santa Fe, NM, USA*
[8]*Center for Environmental Studies, Aspen, CO, USA*
Correspondence: E-mail: noah@alumni.amherst.edu

North American forest growth rates over the 21st century. While inferences drawn from use of historical data sets should be subject to heightened scrutiny when projecting future climates (Williams & Jackson 2007), tree-ring records calibrated against 20th century instrumental records have been successfully used to infer climate patterns thousands of years into the past (Büntgen *et al.* 2011; Trouet *et al.* 2013). We use these climate-growth relationships to project growth changes in the near future, complementing predictions made by vegetation models and environmental niche models. Within this framework, we examined the influence of shifting growth-climate relationships as well as that of enhanced WUE.

METHODS

Vulnerability to climate change can be assessed using two kinds of information: an organism's sensitivity to climate and its projected exposure to climate change (Dawson *et al.* 2011). Accordingly, we combined estimates of how tree growth responds to climate (sensitivity) with estimates of how climate will change in the future (exposure) to forecast how climate change may impact tree growth. Our detailed analytical workflow is summarised with a mathematically defined relationship for each location on the landscape (Fig. 1). We refer to this as the 'perturbation function', because the input is a perturbation in climate and the output is a perturbation in growth. The detailed steps of this process are outlined below.

Assessing climate response

The first step in our forecasting workflow was to characterise the relationship between tree growth and climate. We obtained radial tree growth measurements from 1457 single-species sites in the International Tree Ring Data Bank (ITRDB) and compiled them into a network spanning continental North America (Fig. S3). Each site record consists of data from a single species and was quality checked to ensure (1) a minimum sample of five trees, (2) a minimum signal-to-noise ratio of 0.85, that is, expressed population signal (Wigley *et al.* 1984), and (3) full coverage from 1901 to 1950 CE, the period over which the most tree-ring records were available (Supplementary Methods Note 1). The ITRDB offers limited information on community structure and demography, as well as on the sampling schemes that were applied, but a recent analysis suggested that growth-climate relationships are relatively insensitive to the choice of the sampling scheme at a given site (Nehrbass-Ahles *et al.* 2014). The final network included 1240 coniferous site records and 217 broadleaf site records, with the following dominant genera: *Pinus* ($n = 519$), *Picea* ($n = 245$), *Pseudotsuga* ($n = 218$), Quercus ($n = 204$), *Tsuga* ($n = 112$), *Taxodium* ($n = 28$), *Juniperus* ($n = 26$), *Cedrus* ($n = 23$), and *Larix* ($n = 12$; see also Table S1). Age-related trends in radial tree growth were removed from each individual tree-ring series at each site to obtain annual 'detrended' growth rates, *d,* for each site (Supplementary Methods Note 2).

At each site, we assessed trees' response to climatic variation by correlating *d* with climate records over the period 1900–1950. For this purpose, we obtained the Climatic Research Unit (CRU) 3.21 gridded monthly temperature (T)

and precipitation (P) data at 0.5° spatial resolution (Mitchell & Jones 2005). These data were downscaled to a resolution of 1 km using the WorldClim database of climate normals as a base topography to improve the representation of site climate, particularly in complex terrain (Babst *et al.* 2013). Pearson correlation coefficients were calculated between March of the previous year and August of the current year to account for contemporary and lagged growth responses (36 correlations in total: T correlations for 18 months and P correlations for 18 months). The climate response at each site was defined as the combination of the 36 correlations, $corr(d, c_i)$, between *d* and the focal climate variable, c_i.

To identify the principal types of climate responses in North American forests, we split the 1457 sites into 13 groups according to their monthly climate correlations using a neural network clustering algorithm based on self-organising maps (Supplementary Methods Note 4). The number of groups was set *a priori* to equal the number of ecoregions represented by at least 20 sites in the tree-ring network, but a sensitivity analysis (exploring *a priori* choices of 1, 2, 4, 9, 12, 13, 16, 20 and 25 groups) showed that our conclusions are largely insensitive to this choice (Supplementary Methods Section 10). We tested for statistical significance of the groups using a nonparametric randomisation test (Supplementary Methods Section 9) before averaging the monthly climate correlations of the sites that constitute each group. This resulted in 13 types of climate responses.

Mapping climate response zones

Next, we projected the 13 climate responses across a raster map of the entire landscape of North America, yielding 13 spatially defined climate response zones. To do so, we used climate data extracted at the tree-ring sites (19 bioclimatic variables derived from CMIP5 climate projections averaged over 1900–1950) to predict climate response (1 through 13) as a categorical response variable in a Random Forest analysis (Supplementary Methods Note 5). The fitted Random Forest model was then used to assign each 0.5° grid cell to a climate response zone – once based on 1900–1950 climate normals, and once based on 2051–2099 climate normals. The resulting two maps of historic and future zones describe how the growth of trees in every cell on the landscape is expected to respond to climate variation.

Projecting change in tree growth

Lastly, we combined our climate response zone maps with predicted climate change to forecast the impacts of climate change on tree growth. The growth-climate correlations for each of the 13 zones are treated as local slopes along a global response curve where growth rate (G) is on the y-axis and climate (C) is on the x-axis (Fig. 2). Multiplying the projected change in climate (ΔC) by the local slope ($\frac{dG}{dC}$) provides an estimate of projected change in growth rate (ΔG), limited by the approximation that the tangent characterises the local curve. We capture global nonlinearity of tree growth response to climate by parsing climate space into 13 different zones, each with different characteristic local slopes. In practice, the
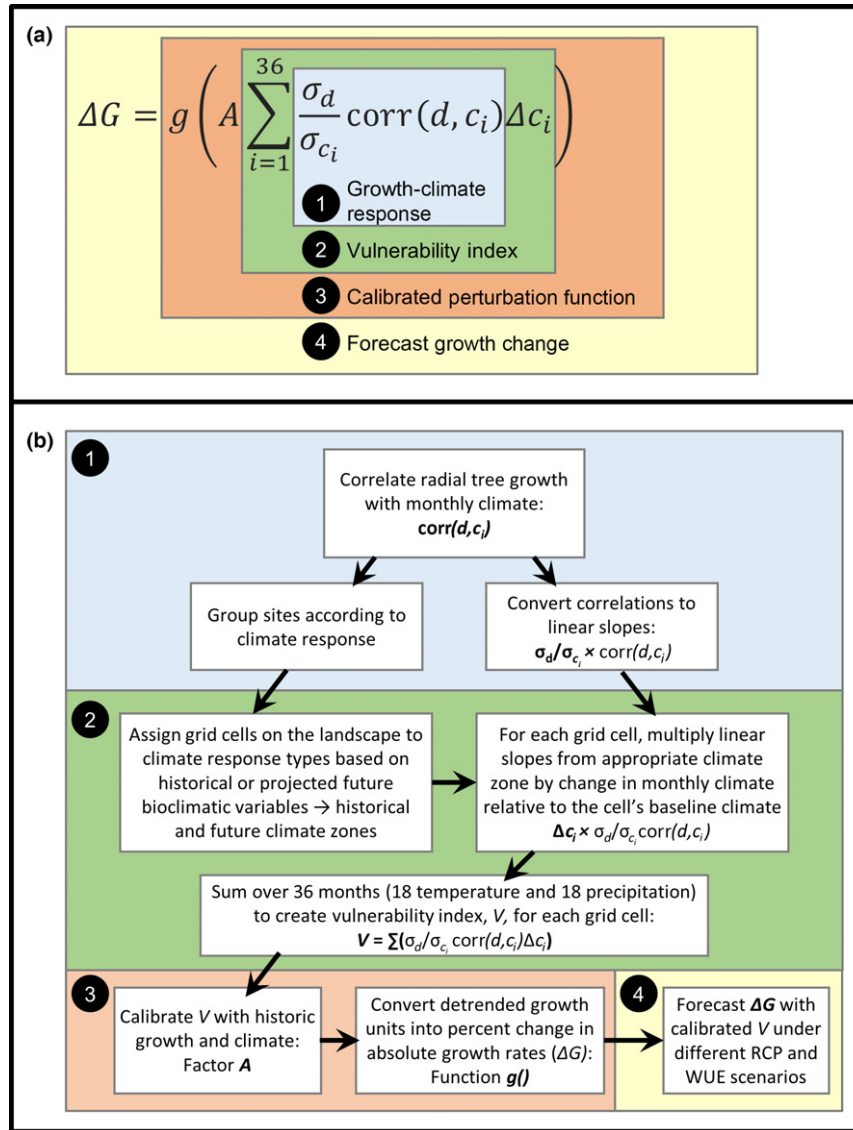
Figure 1 (a) Equation for forecasting changes in tree growth rates based on climate change, where c_i corresponds to one of the 36 (previous March through current August) monthly temperature and precipitation values, d represents the site-level annual detrended tree-ring chronology anomaly values, $corr(d, c_i)$ is the Pearson correlation coefficient between d and c_i, σ_d is the standard deviation of detrended growth rate, $\sigma_{(c_i)}$ is the standard deviation of the focal climate value, Δc_i is the projected difference in the mean of the focal climate value, A, is the slope from a linear regression between hindcast vulnerability index values and observed d, and the function $g()$ converts changes in detrended growth values to percent change in absolute ring width. Numbered boxes correspond to the numbered steps in our (b) workflow for parameterising and applying the equation. We (1) calculate growth-climate correlations, (2) convert these to linear slopes and sum over all 36 climate axes to produce an un-calibrated vulnerability index, and (3) calibrate and convert the output into meaningful units of (4) forecast growth change, which we calculate at each location on the landscape under varying assumptions and climate change scenarios.

climate space is multi-dimensional and the projections require calibration, as detailed below.

A key principle behind our approach is that forecasts are *relative*, based on differences, not absolute values (Fig. 2). We project the *change* in growth for a point on the landscape based upon the co-located *change* in climate, without needing to model the absolute growth, allowing us to make inferences across the entire landscape. To accomplish this, we combined slopes from multiple climate dimensions without including intercepts, as required in a standard multiple-linear regression. This enabled us to incorporate sites from across a broad climatic gradient into the construction of perturbation functions

for each zone and then apply these functions across the gradient.

To project change in tree growth for a given cell on the landscape, we generated a 'vulnerability index,' V (step 2 in Fig. 1). For this purpose, the monthly Pearson correlations that constitute the climate response for a zone were (1) converted to linear slopes through multiplication with the ratio of the standard deviations: $\frac{\sigma d}{\sigma c_i} corr(d, c_i)$, (Supplementary Methods Note 6); (2) multiplied by the projected change in the respective climate variables Δc_i; and (3) summed across all 36 monthly climate variables, yielding $V = \sum_{i=1}^{36} \frac{\sigma d}{\sigma c_i} corr(d, c_i) \Delta c_i$.
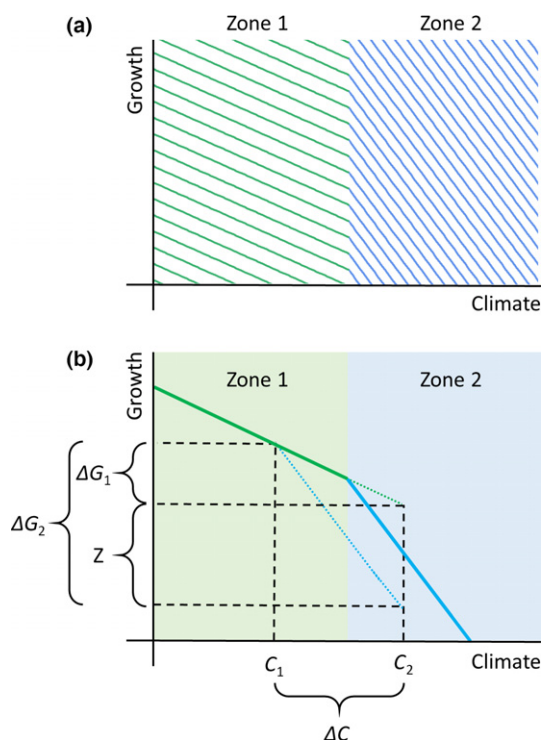
Figure 2 (a) Climate response zones in our model are characterised by distinct linear relationships between growth rates and climate. We do not assume a set intercept for the relationship, but rather a family of parallel lines within each zone. When climate change forces movement through this space, movement occurs parallel to these lines. (b) Our model takes these slopes and uses them to predict change in growth rates (ΔG) from change in climate (ΔC). In any forecast, we can either use the slope of the relationship from the historic zone (zone 1; green line), or the slope of the relationship from the future zone (zone 2; blue line). The best estimate for change in growth is expected to be bounded by ΔG_1 and ΔG_2, thus, we make use of the mean of these values for our final forecast. Across a large population of raster cells randomly distributed with respect to zone boundaries, the mean of this approximation should approach the true global mean. The difference between ΔG_1 and ΔG_2 (Z) is a relative measure of the importance that a changing growth-climate relationship has on the model forecasts.

The vulnerability index V was generated for each grid cell on the landscape. This describes the impact of potential climate change on tree growth in units that are not inherently meaningful – they require calibration. To translate V into ecologically relevant units, we first converted to detrended growth rates using the coefficient A, defined as the slope from a linear regression between hindcast V values and observed d over the 1901–1950 period (Supplementary Methods Note 7). We then converted the detrended growth values to percent change in absolute ring width using the data-derived function $g()$ (see step 3 in Fig. 1 and Supplementary Methods Note 8). We parameterised $g()$ using all consecutive year-pairs during the historical fitting period and the corresponding ring widths for all individual trees at every site. After applying A and $g()$ to V, the output was percent change in radial growth rates in each grid cell (step 4 in Fig. 1).

Combined, the workflow can effectively be described as a perturbation function defined separately for each climate

response zone. Given a difference in climate calculated between two points in time at a given location (ΔC) and the perturbation function for the zone associated with that location (f), we project the percent difference in absolute radial growth rates expected for a tree of any size growing under the two climatic conditions (ΔG) as: $\Delta G = f(\Delta C)$. In full, a zone's perturbation function is thus defined as

$$f(\Delta C) = g\left(A \sum_{i=1}^{36} \frac{\sigma_d}{\sigma_{c_i}} corr(d, c_i) \Delta c_i \right)$$

All parameters are zone-specific, except for the parameters forming the function, $g()$, which is a common conversion defined globally across the tree-ring network.

Recognising that a grid cell may be assigned to a different climate response zone historically compared to the future, we can apply either the perturbation function associated with the historic (f_H) or future (f_F) climate in that cell when calculating ΔG. Future projections based on the historic perturbation function, $f_H(\Delta C)$, neglect changing climate-growth relationships (Fig. 2b, ΔG_1). However, projections based on the future perturbation function, $f_F(\Delta C)$, likely over-estimate the contribution of changing climate-growth relationships (Fig. 2b, ΔG_2). We thus used the mean of the function outputs as our best estimate for growth change incorporating changes in climate-growth relationships. Finally, to estimate mean growth changes across the entire continent, we weighted forecasted growth change in each grid cell by the cell's geographic area and percent forest cover derived from MODIS data prior to averaging.

Simulating a theoretical water-use efficiency enhancement

To incorporate uncertainty due to potential CO_2 fertilisation effects in our tree growth forecasts, we used a first-order approximation approach examining a range of theoretical WUE enhancements. As a combined measure, WUE measures the amount of carbon uptake per unit of water loss without distinguishing the underlying components. Because plants actively control their stomata to optimise carbon gain while minimising water loss, elevated atmospheric CO_2 may lead to reduced stomatal opening (Lin *et al.* 2015). The stomatal closure, combined with the capacity for increased assimilation rates at higher CO_2 concentrations, is predicted to cause smaller increases in the leaf-internal CO_2 concentrations relative to the magnitude of external CO_2 increases, while simultaneously reducing water loss (Keenan *et al.* 2013).

Whether increasing WUE is consistent with water savings via reductions in stomatal conductance, or consistent with increased growth from CO_2 fertilisation, is an active area of research. While there is evidence from flux towers and tree-ring records that plants have become more water-use efficient (Frank *et al.* 2015), additional evidence from experimental and observational work suggests an increase in water savings that can be obscured by climate change and changes in plant form (e.g. increases in leaf area index) that counter water savings at the leaf level (Norby & Zak 2011). Observations of increased soil moisture in free-air CO_2 experiments (Leuzinger & Koerner 2007) and increased continent-wide runoff

(Gedney *et al.* 2006) suggest that leaf-level responses are scalable to stand-level hydrologic dynamics. Thus, increase in water availability, be it actual or effective, with increasing CO_2 appears at least plausible based on available evidence. We therefore built enhanced WUE as an unresolved hypothesis within our forecasting workflow.

Farquhar (1997) formulated an approximation for enhanced WUE, finding that '*doubling the $CO2$ concentration is almost like doubling the rainfall as far as plant water availability is concerned.*' Donohue *et al.* (2009) later used this approach as part of their analysis of climate-related trends in Australian vegetation. Following this theory, we modelled enhanced WUE as a proportionate increase in effective precipitation. In application, this approach assumes that water-limited plants are also carbon-limited, and vice versa, because stomatal conductance couples CO_2 uptake with water loss. Thus, an increase in atmospheric CO_2 elicits the same response as would an increase in water availability. Because we manipulate precipitation in the simulations, we assume that a change in precipitation causes a proportionate change in water available to the focal trees. This approach furthermore assumes that the observed growth-precipitation correlations represent a real causal link between precipitation and growth. We thus note that our treatment of WUE should be regarded as scenarios conditioned upon the above assumptions and limitations.

We implement WUE enhancement scenarios by multiplying future precipitation inputs by a scaling factor prior to projecting future zone distributions and prior to applying the perturbation functions. For instance, if a given grid cell is forecast to have an average of 2 cm of January precipitation under future climates, in scenarios where we enhance WUE by 50%, we would scale the future January precipitation in that cell to 3 cm prior to forecasting growth changes. For cells in zones with weak correlations between precipitation and tree growth, this modification should have little impact on growth forecasts. However, in zones with strong precipitation responses, increasing effective precipitation should have a large impact on growth forecasts.

To understand the sensitivity of growth forecasts to WUE, we stepped through various scenarios for simulated WUE increases for each future representative concentration pathway (RCP) scenario ranging from 0% increase to 150% increase in WUE in 1% interval steps. The upper limit for WUE enhancement would be an increase proportional to the percent increase in atmospheric CO_2 (Medlyn *et al.* 2011). Comparing mean CO_2 concentrations during the historic and future time periods, the four RCP scenarios 2.6, 4.5, 6.0, and 8.5 respectively project 42, 72, 88, and 137% increases in CO_2 (http://tntcat.iiasa.ac.at/RcpDb). We take these percent increases to be the upper limits for potential WUE enhancement under the four RCP scenarios assuming a directly linear response.

RESULTS

Spatial projections of the 13 climate response zones for the 1901–1950 period confirm well-known gradients (Babst *et al.* 2013), with strong precipitation limitation of tree growth in hot and dry regions and temperature limitation in cold and humid regions (Fig. 3b). With no WUE feedback, our projection for 2051–2099 based on a business-as-usual greenhouse gas emission scenario (RCP 8.5) indicates a dramatic northward expansion of the most precipitation-limited zones (i.e. zones 10–13; Fig. 3c) as far as interior Alaska. Averaged across the 18 months and then across the 13 zones, the mean temperature-growth correlations were -0.029 (SD = 0.058, $n = 13$), while the mean precipitation-growth correlations were 0.072 (SD = 0.057, $n = 13$). Although these correlations are similar orders of magnitude, with a slightly stronger precipitation response, the projected future change in temperature is much larger than the projected future change in precipitation; the mean ratio of projected change divided by historical annual variance is 28 times larger for temperature than for precipitation. Thus, in concurrence with other studies, the increase in water limitation is attributable primarily to long-term increased temperature and associated evaporative demand, rather than reduced precipitation (Williams *et al.* 2012). After weighting by MODIS forest cover data, we project that 57% of the forested North American land surface shifts to a new climate response zone by the end of the 21st century, and that the area characterised by temperature-limited tree growth (zones 1–2) will decrease from 1.7 million km^2 to 0.5 million km^2 (Fig. S5c). When we simulated extreme WUE increases of 137%, we project contraction of both the most water-limited and most temperature-limited climate zones, and expansion of the climate zones that currently characterise most of the eastern half of the continent (zones 7 and 9, Fig. 3d), with a shift in zones across 61% of the forested landscape (Fig. S5d).

Comparing projections based on static growth-climate relationships (f_H) with projections that allow grid cells to shift climate response zones (f_F), shifts in climate-growth relationships modulated or even reversed growth changes expected from climate change alone. This effect was most pronounced in temperature-limited zones under constant WUE assumptions (zones 1–2, Fig. 4; Fig. S6), where, with static climate-growth relationships, growth was otherwise projected to increase (i.e. 'boreal greening'; Alcaraz-Segura *et al.* 2010). Under both the enhanced and static WUE scenarios, we projected growth declines or stasis across much of the central, western and boreal regions of North America (Fig. 5). Some of the regions with the strongest expected growth declines are places where forests currently exist at their dry limits (Allen *et al.* 2010). This was contrasted by higher growth rates along the Pacific coast, the Gulf of Mexico and in northeastern Canada. Extreme enhancement of WUE (+137%) accelerated growth in these areas where growth increased under the static WUE scenario, while simultaneously reversing the growth declines projected under the static WUE scenario across much of the eastern United States (Fig. 5e).

In the absence of increased WUE, changes in temperature and precipitation were forecast to cause a continent-wide average growth decline between -6.3% (RCP 2.6; SD = 3.4%) and -19.4% (RCP 8.5; SD = 8.1%). It took a 72% increase in WUE to balance the projected growth declines under RCP 8.5 (Fig. 5f). Under the extreme scenario that WUE increased in proportion to CO_2, average continental growth increased between 2.4% (RCP 2.6; SD = 2.9) and
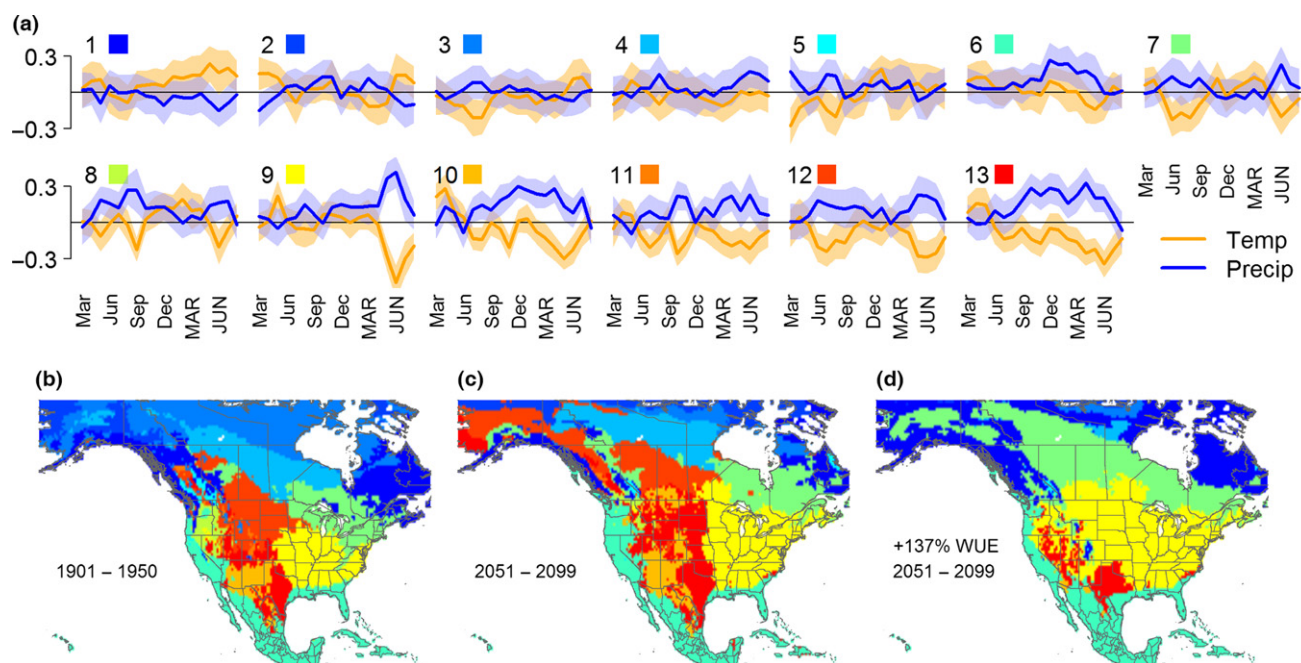
Figure 3 Projected spatial distribution of 13 climate response zones across North America. (a) The mean monthly correlation between detrended tree-ring width and temperature (orange) and precipitation (blue) in each of 13 climate response zones (plus and minus standard deviations, shaded). Months from the current year are denoted with capitalised letters. (b) Spatial projection of each of the climate response zones during the fitting period, 1901–1950, (c) for 2051–2099 assuming static water-use efficiency (WUE), and (d) for 2051–2099 assuming WUE increases in proportion to increased CO_2, given RCP scenario 8.5, with colours corresponding to swatches in (a). Zones are ordered by the relative strength of temperature and precipitation correlations.
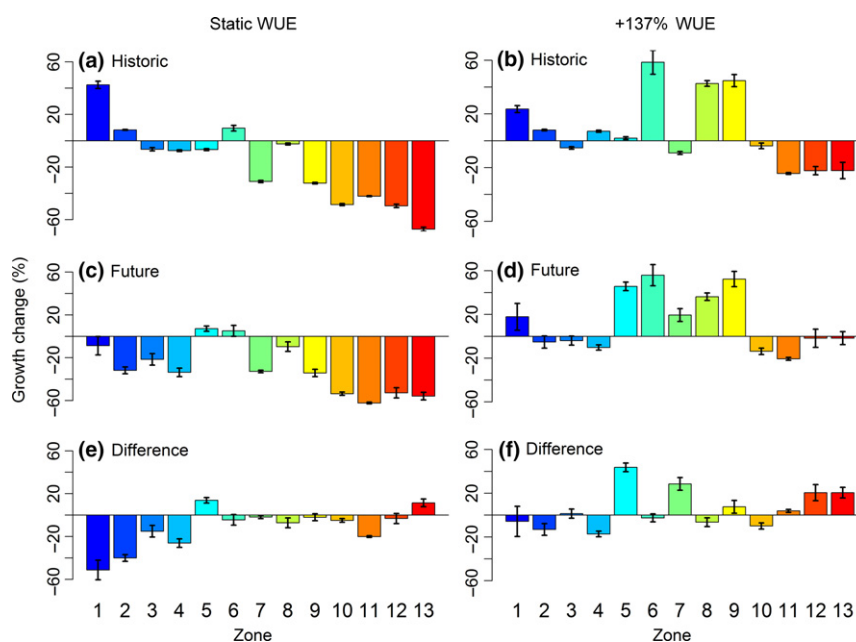

Figure 4 Projected tree growth change in 13 climate response zones spanning North America based on (a and b) historic climate-growth relationships, (c and d) future climate-growth relationships and (e and f) the difference between these projections assuming static WUE (left) or 137% increased WUE (right). Bar heights represent means weighted by the land area and percent forest within each cell. Error bars represent standard deviations. For each zone, the historic, future and difference bars represent the same set of cells identified by their historic zone assignment.

17.0% (RCP 8.5; SD = 8.0; Fig. S11). Examining spatial variance in climate change impacts, the standard deviation in projected growth change across grid cells increased between RCP 2.6 and RCP 8.5 by factors of 2.4 and 3.0 for the constant WUE and full WUE enhancement models, respectively (Fig. 5c).
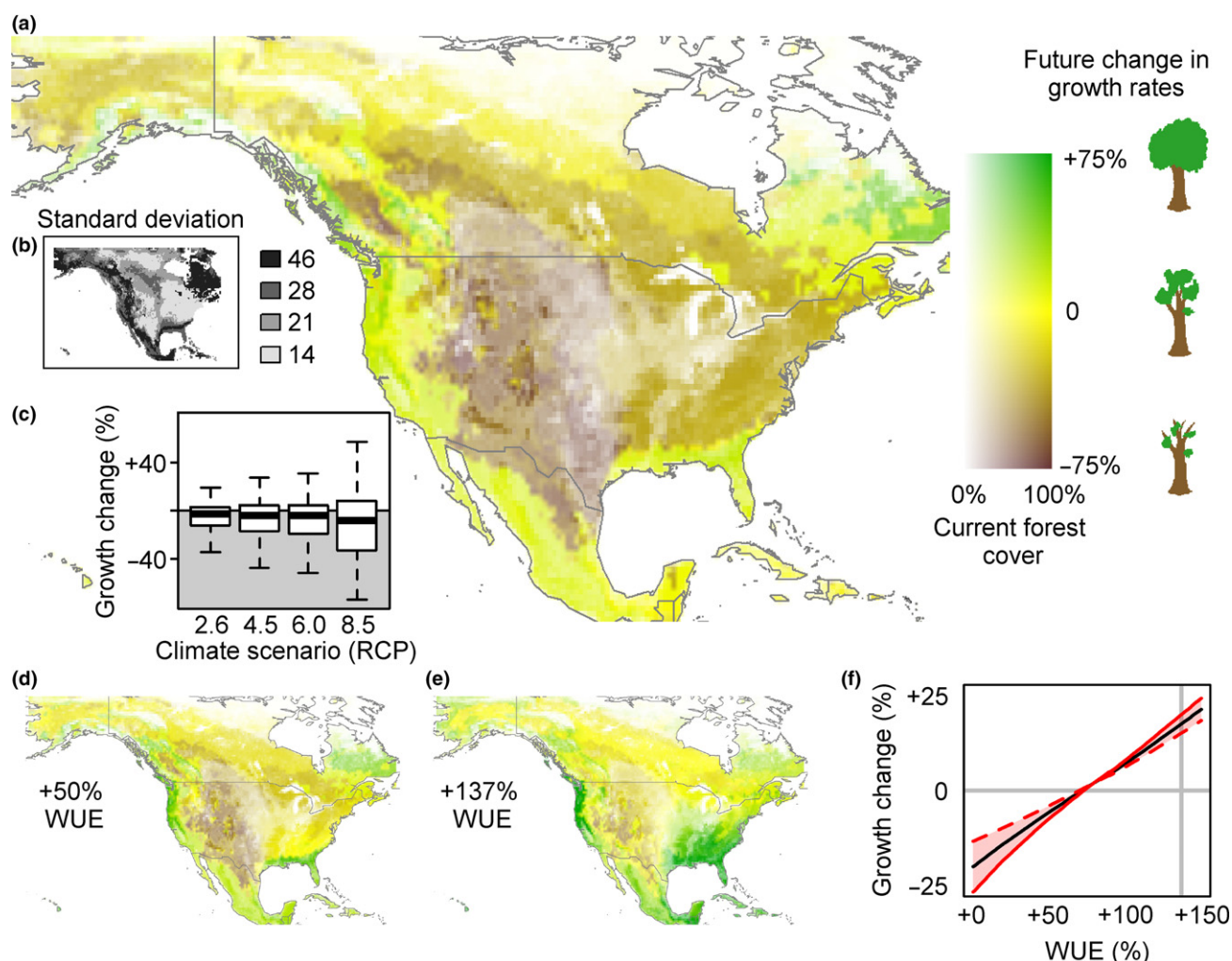
Figure 5 (a) Projected change in tree growth rates due to climate change under RCP 8.5 assuming no increase in water use efficiency (WUE). Values represent the percent difference in diameter growth rates expected for a tree growing under the climate projected for the last half of the 21st century compared to a comparable tree in a comparable ecological context under the climate observed at that location in the first half of the 20th century. (b) Standard deviations are calculated across all forecast trials and individual GCMs under RCP 8.5 with no increase in WUE. (c) Boxplot provides the distributions of growth change on a cell-by-cell basis for four different climate scenarios. Small maps show projections adjusted by an increase in WUE of (d) 50% and (e) 137%, which is equal to projected CO_2 increases. (f) Line plot shows growth change as a function of WUE enhancement, where the dotted red line gives projections based on historic zones (f_H), solid red line is based on future zones (f_F), black line is the mean, and the vertical grey line is 137% increase in WUE.

DISCUSSION

This study provides new empirically based constraints on modelled climate-induced changes in forest growth across North America and represents a novel approach by considering geographic shifts in climate response zones in 21st century forecasts. This is an important advance in quantifying ecological responses to climate change, because, although it is acknowledged that ecosystem vulnerability to climate change depends on both climate forcing and organismal response, adequately incorporating shifting sensitivities remains a major challenge (Dawson *et al.* 2011). The observed differences between projections with and without shifting climate sensitivities (f_F vs. f_H) demonstrate the significance of this effect. Our zone-mapping technique, hence, provides a framework that other researchers can use to better integrate geographic variation in species ecologies into climate change models while accounting for intraspecific variation. Regional differences in the direction of projected growth declines and enhancements are particularly relevant for forest monitoring, management and research. In addition, the varying magnitude of the projected continental-scale decline in forest growth among the four RCP scenarios (Fig. 5c) underscores the importance of continued efforts to limit global greenhouse gas emissions (Boyd *et al.* 2015).

An important finding of this study is that over half of the forested land in North America shifted climate response zones, with most of that area shifting towards stronger precipitation limitation. Our projections are supported by recent observations that high-latitude forests are shifting from temperature-limited growth to precipitation-limited growth in areas where we project this pattern (Juday *et al.* 2015;

Marcinkowski *et al.* 2015), which suggests that CO_2-driven WUE feedbacks will become increasingly important. This is particularly relevant for tree mortality algorithms used in dynamic global vegetation models, which would benefit from greater clarity of the relative importance of temperature and precipitation on tree mortality (McDowell *et al.* 2011). Indeed, Williams *et al.* (2012) identified uncertainty in the relative importance of evaporative demand vs. precipitation to tree mortality as a major barrier to our ability to forecast the future fates of forests using global climate model output. Most reports of drought-induced tree mortality come from low- and mid-latitude tropical and temperate forests, but recent work has indicated that North American boreal forests have also experienced drought-induced mortality in the last half century (Peng *et al.* 2011). In our forecasts of boreal forests, the shift from temperature limitation to precipitation limitation was a major driver of declining growth rates. The fate of boreal forests has been identified as critical to a tipping point in the Earth's global carbon cycle (Lenton *et al.* 2008). Thus, our forecasts that they may become negatively sensitive to temperature, together with evidence suggesting this transition is already happening (Juday *et al.* 2015), underscores the potential for this current carbon sink to become a source.

Species' phenotypes vary widely across their ranges as a result of exposure to divergent environments. Thus, differences in tree growth are often driven more by site-level differences than species-level differences (Fritts 1974; Martin-Benito & Pederson 2015). Accordingly, we use a tree's location in climate space to predict the climate response without explicit reference to the species identity. The results of our cluster analysis support the use of models that emphasise intraspecific variation, as species were widely distributed among the climate response groups (Table S1). There were 11 species that exhibited at least 7 of the 13 climate response types, and these 11 species represent 52% of sites. The most abundant species in our data set, *Pinus ponderosa* (Douglas ex C. Lawson), exhibited 10 of the 13 climate response types. As a consequence, 81% of *P. ponderosa* sites are projected to experience growth declines (up to −70% growth; on average −50% growth), whereas 19% of *P. ponderosa* sites are projected to experience growth increases (up to +27% growth; on average +11% growth). This same basic pattern, of a single species exhibiting divergent climate responses, was found for most of the dominant species in our network. This contrasts with frameworks such as ecological niche modelling, in which species are often treated as homogenous units (Gotelli & Stanton-Geddes 2015).

Because our model implies a global underlying climate-growth response surface for all trees, projected shifts in the geographic distribution of climate response zones do not imply similar shifts in the species' geographic distributions. The time frame of our projections is relatively short compared to the time required for new tree species to colonise and dominate forests in other zones. To the extent that populations exhibit adaptations to their local climate, as opposed to phenotypically-plastic climate responses, the standing composition of forests is likely to be maladapted for projected 21st century climate conditions. The likely implication is that actual declines in tree growth rates would be greater than those forecast here.

In our explorations of WUE enhancement, the importance of this effect varied depending on climate response zone and, as expected, was generally most important in more water-limited zones. Yet this effect, represented via an increase in effective precipitation (Farquhar 1997), remained insufficient to reverse projected growth declines across much of North America (e.g. zones 4, 10–13 Fig. 4; Fig. S1), even with the unlikely upper-limit scenario under which WUE increased proportionally with CO_2 (Medlyn *et al.* 2011). The advantage of our approach to simulating WUE enhancement is that it does not treat all ecosystems in a similar manner. Rather, increased effective precipitation results in greater growth enhancement in more drought-stressed ecosystems, consistent with theoretical and observational lines of evidence (Donohue *et al.* 2013). The limitations of our approach are evident in the most temperature-limited zone (Fig. 4, zone 1) where the observed growth-precipitation correlations are slightly negative. These negative correlations cause an unrealistic decrease in growth associated with increased WUE for 5.6% of the forest-weighted landscape (Fig. 5e). Thus, our implementation of increased WUE should be viewed as an imperfect but useful first-order approximation of potential effects. As a sensitivity analysis implemented across a wide range of WUE scenarios, this contributes to an area of active debate, in which a significant body of literature highlights uncertainties in the capacity for increased WUE to translate directly into increased growth rather than water savings (Allen *et al.* 2015; Frank *et al.* 2015). This includes empirical observations of enhanced WUE failing to translate into enhanced growth (van der Sleen *et al.* 2014), nutrient limitations that dampen WUE effects (Norby *et al.* 2010) and the inability of increased atmospheric CO_2 to prevent drought-induced mortality (Allen *et al.* 2010; Duan *et al.* 2014).

Underlying observed climate-growth relationships are a complex set of physiological processes governing the responses of tree growth to drought and heat stress. Although directly modelling growth may provide more mechanistically based projections, these processes are confounded by high uncertainties due to complexities with varying degrees of representation in current models (Fatichi *et al.* 2014). Differences in how factors such as stomatal regulation are parameterised in mechanistic models contribute to radically different estimates of terrestrial carbon cycling (Friedlingstein *et al.* 2006). Our approach offers a phenomenologically based complement to these mechanistic models. Uncertainty analyses (Supplementary Methods Note 10) demonstrate good precision, allowing us to have confidence in the regional patterns, the effect of shifting sensitivities and comparisons among various RCP scenarios. It is more difficult to assess systematic biases that may reduce forecast accuracy and thus alter the magnitude of absolute estimates. For instance, spatial projections of climate response zones could be complicated by missing covariates such as geology, soils or other spatially autocorrelated factors (Record & Charney 2016). Furthermore, dendroclimatological site selection may bias results by emphasising those trees that are most sensitive to climate (Babst *et al.* 2014).

A persistent problem confronting climate change forecasting is that future climates may have no analogue in the historical data (Williams & Jackson 2007). Our space-for-time substitution approach coupled with the ability of trees to shift their

sensitivities in our modelling framework partially addresses this problem. Given the continent-wide scale of our analysis, the values of all 19 individual bioclimatic variables used to project climate response zones fall within the range of values represented in the historical fitting data for 96% of cells under the most extreme RCP forecast.

In examining direct effects of climate on growth, we capture just one component of the ultimate fate of forests, which will also depend upon the frequency and intensity of extreme events (Reichstein *et al.* 2013), stand demography (Stephenson *et al.* 2014), disturbances such as wildfire and pathogen outbreaks (Millar & Stephenson 2015) and management practices (Carpenter *et al.* 2009). While many forces will shape trees of the future, an analysis based on temperature and precipitation impacts offers an important baseline for predicting the underlying limits of future growth (Choat *et al.* 2012). Our projections highlight forested areas of particular vulnerability to climate change (e.g. areas of continental climates in western interior North America), which are consistent with predictions from other studies using different methods to locate where forest stress and mortality linked to climate change will likely be most severe (Allen *et al.* 2010; Williams *et al.* 2012). Following the 21st Conference of the Parties (COP21), where 196 nations unanimously committed to take steps to address climate change, there is an increasing understanding of the need to manage the carbon cycle on a planetary scale. For most of recent history, forests have played a significant role mitigating the effects of greenhouse gas emissions. However, the possibility that rising temperatures may shift large swaths of forest towards negative growth-temperature correlations represents a feedback loop with the potential to accelerate climate change beyond critical tipping points.

AUTHORSHIP

NDC, FB and MEKE conceived of main analyses. FB and BP compiled data. NDC performed analyses and generated main figures. All authors contributed to intellectual project development and paper writing.

REFERENCES

Ainsworth, E.A. & Long, S.P. (2005). What have we learned from 15 years of free-air CO2 enrichment (FACE)? A meta-analytic review of the responses of photosynthesis, canopy properties and plant production to rising CO_2. *New Phytol.*, 165, 351–372.

Albright, W.L. & Peterson, D.L. (2013). Tree growth and climate in the Pacific Northwest, North America: a broad-scale analysis of changing growth environments. *J. Biogeogr.*, 40, 2119–2133.

Alcaraz-Segura, D., Chuvieco, E., Epstein, H.E., Kasischke, E.S. & Trishchenko, A. (2010). Debating the greening vs. browning of the North American boreal forest: differences between satellite datasets. *Glob. Chang. Biol.*, 16, 760–770.

Allen, C.D., Macalady, A.K., Chenchouni, H., Bachelet, D., McDowell, N., Vennetier, M. *et al.* (2010). A global overview of drought and heat-induced tree mortality reveals emerging climate change risks for forests. *For. Ecol. Manage.*, 259, 660–684.

Allen, C., Breshears, D. & McDowell, N. (2015). On underestimation of global vulnerability to tree mortality and forest die-off from hotter drought in the Anthropocene. *Ecosphere*, 6, 1–55.

Babst, F., Poulter, B., Trouet, V., Tan, K., Neuwirth, B., Wilson, R. *et al.* (2013). Site- and species-specific responses of forest growth to climate across the European continent. *Glob. Ecol. Biogeogr.*, 22, 706–717.

Babst, F., Alexander, M.R., Moore, D.J., Monson, R., Frank, D.C., Klesse, S., Bouriaud, O., Poulter, B., Ciais, P., Roden, J., Trouet, V. (2014). A tree-ring perspective on the terrestrial carbon cycle. *Oecologia* DOI 10.1007/s00442-014-3031-6.

Blois, J.L.J.L., Williams, J.W.J.W., Fitzpatrick, M.C.M.C., Jackson, S.T. & Ferrier, S. (2013). Space can substitute for time in predicting climate-change effects on biodiversity. *Proc. Natl Acad. Sci.*, 110, 9374–9379.

Bonan, G.B. (2008). Forests and climate change: forcings, feedbacks, and the climate benefits of forests. *Science*, 320, 1444–1449.

Boyd, R., Turner, J. & Ward, B. (2015). *Intended Nationally Determined Contributions: What are the Implications for Greenhouse Gas Emissions in 2030?*. Centre for Climate Change Economics and Policy, Grantham Research Institute on Climate Change and the Environment, London.

Büntgen, U., Tegel, W., Nicolussi, K., McCormick, M., Frank, D., Trouet, V. *et al.* (2011). 2500 years of European climate variability and human susceptibility. *Science*, 331, 578–582.

Carpenter, S.R., Mooney, H.A., Agard, J., Capistrano, D., Defries, R.S., Díaz, S. *et al.* (2009). Science for managing ecosystem services: beyond the Millennium ecosystem assessment. *Proc. Natl Acad. Sci. USA*, 106, 1305–1312.

Choat, B., Jansen, S., Brodribb, T.J., Cochard, H., Delzon, S., Bhaskar, R. *et al.* (2012). Global convergence in the vulnerability of forests to drought. *Nature*, 491, 752–755.

Dawson, T.P., Jackson, S.T., House, J.I., Prentice, I.C. & Mace, G.M. (2011). Beyond predictions: biodiversity conservation in a changing climate. *Science*, 332, 53–58.

Donohue, R.J., McVICAR, T.I.M. & Roderick, M.L. (2009). Climate-related trends in Australian vegetation cover as inferred from satellite observations, 1981–2006. *Glob. Chang. Biol.*, 15, 1025–1039.

Donohue, R.J., Roderick, M.L., McVicar, T.R. & Farquhar, G.D. (2013). Impact of CO_2 fertilization on maximum foliage cover across the globe's warm, arid environments. *Geophys. Res. Lett.*, 40, 3031–3035.

Duan, H., Duursma, R.A., Huang, G., Smith, R.A., Choat, B., O'Grady, A.P. *et al.* (2014). Elevated [CO_2] does not ameliorate the negative effects of elevated temperature on drought-induced mortality in *Eucalyptus radiata* seedlings. *Plant, Cell Environ.*, 37, 1598–1613.

Farquhar, G.D. (1997). Carbon dioxide and vegetation. *Science*, 278, 1411.

Farrior, C.E., Rodriguez-Iturbe, I., Dybzinski, R., Levin, S.A. & Pacala, S.W. (2015). Decreased water limitation under elevated CO_2 amplifies potential for forest carbon sinks. *Proc. Natl Acad. Sci.*, 112, 7213–7218.

Fatichi, S., Leuzinger, S. & Körner, C. (2014). Moving beyond photosynthesis: from carbon source to sink-driven vegetation modeling. *New Phytol.*, 201, 1086–1095.

Frank, D.C., Poulter, B., Saurer, M., Esper, J., Huntingford, C., Helle, G. *et al.* (2015). Water-use efficiency and transpiration across European forests during the Anthropocene. *Nat. Clim. Chang.*, 5, 579–583.

Friedlingstein, P., Cox, P., Betts, R., Bopp, L., Von Bloh, W., Brovkin, V. *et al.* (2006). Climate-carbon cycle feedback analysis: results from the C^{4}MIP model intercomparison. *J. Clim.*, 19, 3337–3353.

Fritts, H. (1974). Relationships of ring widths in arid-site conifers to variations in monthly temperature and precipitation. *Ecol. Monogr.*, 44, 411–440.

Gedney, N., Cox, P.M., Betts, R.A., Boucher, O., Huntingford, C. & Stott, P.A. (2006). Detection of a direct carbon dioxide effect in continental river runoff records. *Nature*, 439, 835–838.

Gotelli, N.J. & Stanton-Geddes, J. (2015). Climate change, genetic markers and species distribution modelling. *J. Biogeogr.*, 42, 1577–1585.

Juday, G.P., Alix, C. & Grant, T.A. (2015). Spatial coherence and change of opposite white spruce temperature sensitivities on floodplains in Alaska confirms early-stage boreal biome shift. *For. Ecol. Manage.*, 350, 46–61.

Keenan, T.F., Davidson, E., Moffat, A.M., Munger, W. & Richardson, A.D. (2012). Using model-data fusion to interpret past trends, and quantify uncertainties in future projections, of terrestrial ecosystem carbon cycling. *Glob. Chang. Biol.*, 18, 2555–2569.

Keenan, T.F., Hollinger, D.Y., Bohrer, G., Dragoni, D., Munger, J.W., Schmid, H.P. *et al.* (2013). Increase in forest water-use efficiency as atmospheric carbon dioxide concentrations rise. *Nature*, 499, 324–327.

Lenton, T.M., Held, H., Kriegler, E., Hall, J.W., Lucht, W., Rahmstorf, S. *et al.* (2008). Tipping elements in the Earth's climate system. *Proc. Natl Acad. Sci.*, 105, 1786–1793.

Leuzinger, S. & Koerner, C. (2007). Water savings in mature deciduous forest trees under elevated CO_2. *Glob. Chang. Biol.*, 13, 2498–2508.

Lin, Y.-S., Medlyn, B.E., Duursma, R.A., Prentice, I.C., Wang, H., Baig, S. *et al.* (2015). Optimal stomatal behaviour around the world. *Nat. Clim. Chang.*, 5, 459–464.

Lindner, M., Fitzgerald, J.B., Zimmermann, N.E., Reyer, C., Delzon, S., van der Maaten, E. *et al.* (2014). Climate change and European forests: what do we know, what are the uncertainties, and what are the implications for forest management? *J. Environ. Manage.*, 146, 69–83.

Marcinkowski, K., Peterson, D.L. & Ettl, G.J. (2015). Nonstationary temporal response of mountain hemlock growth to climatic variability in the North Cascade Range. *Can. J. For. Res.*, 45, 676–688.

Martin-Benito, D. & Pederson, N. (2015). Convergence in drought stress, but a divergence of climatic drivers across a latitudinal gradient in a temperate broadleaf forest. *J. Biogeogr.*, 42, 925–937.

McDowell, N.G., Beerling, D.J., Breshears, D.D., Fisher, R.A., Raffa, K.F. & Stitt, M. (2011). The interdependence of mechanisms underlying climate-driven vegetation mortality. *Trends Ecol. Evol.*, 26, 523–532.

McDowell, N.G., Williams, A.P., Xu, C., Pockman, W.T., Dickman, L.T., Sevanto, S. *et al.* (2015). Multi-scale predictions of massive conifer mortality due to chronic temperature rise. *Nat. Clim. Chang.*, 6, 295–300.

Medlyn, B.E., Duursma, R.A., Eamus, D., Ellsworth, D.S., Prentice, I.C., Barton, C.V.M. *et al.* (2011). Reconciling the optimal and empirical approaches to modelling stomatal conductance. *Glob. Chang. Biol.*, 17, 2134–2144.

Millar, C.I. & Stephenson, N.L. (2015). Temperate forest health in an era of emerging megadisturbance. *Science*, 349, 823–826.

Mitchell, T.D. & Jones, P.D. (2005). An improved method of constructing a database of monthly climate observations and associated high-resolution grids. *Int. J. Climatol.*, 25, 693–712.

Nabuurs, G.-J., Lindner, M., Verkerk, P.J., Gunia, K., Deda, P., Michalak, R. *et al.* (2013). First signs of carbon sink saturation in European forest biomass. *Nat. Clim. Chang.*, 3, 792–796.

Nehrbass-Ahles, C., Babst, F., Klesse, S., Nötzli, M., Bouriaud, O., Neukom, R. *et al.* (2014). The influence of sampling design on tree-ring based quantification of forest growth. *Glob. Chang. Biol.*, 20, 2867–2885.

Norby, R.J. & Zak, D.R. (2011). Ecological lessons from free-air CO_2 enrichment (FACE) experiments. *Annu. Rev. Ecol. Evol. Syst.*, 42, 181–203.

Norby, R.J., Warren, J.M., Iversen, C.M., Medlyn, B.E. & McMurtrie, R.E. (2010). CO_2 enhancement of forest productivity constrained by limited nitrogen availability. *Proc. Natl Acad. Sci. USA*, 107, 19368–19373.

Pan, Y., Birdsey, R.A., Fang, J., Houghton, R., Kauppi, P.E., Kurz, W.A. *et al.* (2011). A large and persistent carbon sink in the world's forests. *Science*, 333, 988–993.

Peng, C., Ma, Z., Lei, X., Zhu, Q., Chen, H., Wang, W. *et al.* (2011). A drought-induced pervasive increase in tree mortality across Canada's boreal forests. *Nat. Clim. Chang.*, 1, 467–471.

Piao, S., Sitch, S., Ciais, P., Friedlingstein, P., Peylin, P., Wang, X. *et al.* (2013). Evaluation of terrestrial carbon cycle models for their response to climate variability and to CO_2 trends. *Glob. Chang. Biol.*, 19, 2117–2132.

Piao, S., Nan, H., Huntingford, C., Ciais, P., Friedlingstein, P., Sitch, S. *et al.* (2014). Evidence for a weakening relationship between interannual temperature variability and northern vegetation activity. *Nat. Commun.*, 5, 5018.

Record, S. & Charney, N.D. (2016). Modeling species ranges. *Chance*, 29, 31–37.

Reichstein, M., Bahn, M., Ciais, P., Frank, D., Mahecha, M.D., Seneviratne, S.I. *et al.* (2013). Climate extremes and the carbon cycle. *Nature*, 500, 287–295.

van der Sleen, P., Groenendijk, P., Vlam, M., Anten, N.P.R., Boom, A., Bongers, F. *et al.* (2014). No growth stimulation of tropical trees by 150 years of CO_2 fertilization but water-use efficiency increased. *Nat. Geosci.*, 8, 24–28.

Stephenson, N.L., Das, A.J., Condit, R., Russo, S.E., Baker, P.J., Beckman, N.G. *et al.* (2014). Rate of tree carbon accumulation increases continuously with tree size. *Nature*, 507, 90–93.

Trouet, V., Diaz, H.F., Wahl, E.R., Viau, A.E., Graham, R., Graham, N. *et al.* (2013). A 1500-year reconstruction of annual mean temperature for temperate North America on decadal-to-multidecadal time scales. *Environ. Res. Lett.*, 8, 024008.

Wigley, T., Briffa, K. & Jones, P. (1984). On the average value of correlated time series, with applications in dendroclimatology and hydrometeorology. *J. Clim. Appl. Meteorol.*, 23, 201–213.

Williams, J.W. & Jackson, S.T. (2007). Novel climates, no-analog communities, and ecological surprises. *Front. Ecol. Environ.*, 5, 475–482.

Williams, A.P., Xu, C. & McDowell, N.G. (2011). Who is the new sheriff in town regulating boreal forest growth? *Environ. Res. Lett.*, 6, 041004.

Williams, A.P., Allen, C.D., Macalady, A.K., Griffin, D., Woodhouse, C.A., Meko, D.M. *et al.* (2012). Temperature as a potent driver of regional forest drought stress and tree mortality. *Nat. Clim. Chang.*, 3, 292–297.

SUPPORTING INFORMATION

Additional Supporting Information may be found online in the supporting information tab for this article.